

Climatology of diurnal tide and its long-term variability in the lower middle atmosphere over a tropical station

P. Vinay Kumar¹ · Gopa Dutta¹ · Salauddin Mohammad
B. Venkateswara Rao²

Received: 10 March 2015 / Accepted: 13 July 2016 / Published online: 25 July 2016
© Springer-Verlag Wien 2016

Abstract ECMWF reanalysis (ERA–interim) data of winds for two solar cycles (1991–2012) are harmonically analyzed to delineate the characteristics and variability of diurnal tide over a tropical site (13.5° N, 79.5° E). The diurnal cycle horizontal winds measured by Gadanki (13.5° N, 79.2° E) mesosphere–stratosphere–troposphere (MST) radar between May 2005 and April 2006 have been used to compute 24 h tidal amplitudes and phases and compared with the corresponding results obtained from ERA winds. The climatological diurnal tidal amplitudes and phases have been estimated from surface to ~33 km using ERA interim data. The amplitudes and phases obtained in the present study are found to compare reasonably well with Global Scale Wave Model (GSWM–09). Diurnal tides show larger amplitudes in the lower troposphere below 5 km during summer and in the mid-stratosphere mainly during equinoctial months and early winter. Water vapor and convection in the lower troposphere are observed to play major roles in exciting 24-h tide. Correlations between diurnal amplitude and integrated water vapor and between diurnal amplitude and outgoing longwave radiation (OLR) are 0.59 and –0.34, respectively. Ozone mixing ratio correlates ($\rho = 0.66$) well with diurnal amplitude and shows annual variation in the troposphere whereas semi-annual variation is observed at stratospheric heights with stronger peaks in equinoctial months. A clear annual variation of diurnal amplitude is displayed in the troposphere and

interannual variability becomes prominent in the stratosphere which could be partly due to the influence of equatorial stratospheric QBO. The influence of solar activity on diurnal oscillations is found to be insignificant.

1 Introduction

Absorption of solar radiation by water vapor in the troposphere and ozone in the stratosphere primarily generate atmospheric tides. These global scale internal waves propagate upward and transfer momentum and energy from their source regions to the upper atmosphere through nonlinear interaction and wave breaking. Numerous theoretical and experimental studies on tidal oscillations have been reported till date, but majority of these studies have addressed the problem in the mesospheric and lower thermospheric (MLT) regions where the amplitudes of these waves are large (e.g., Sasi and Krishnamurthy 1990; Hocking and Hocking 2002; Meek et al. 2011).

Tidal parameters show lot of variability on different time scales from short to interannual periods. It is well established that modulation of gravity waves by tides is responsible for short-term variability of the waves. Nonlinear interaction between tides and planetary waves are also reported to contribute to short-term variations (Fritts and Vincent 1987; Hall et al. 1995; Chang et al. 2011). The long-term variations like the seasonal and interannual variability of diurnal tide have been investigated for a long time in the MLT region (Burrage et al. 1995; Hall et al. 1995; Zhang et al. 2011; Kishore Kumar et al. 2014a). The interannual variability of diurnal tide in MLT region has been linked to quasi-biennial oscillation (QBO) in equatorial stratospheric zonal wind (Vincent et al. 1998). The 24-h oscillation in the low-latitude MLT region has also been reported to be associated with El Niño southern

✉ Gopa Dutta
gopadutta@yahoo.com

¹ Vignana Bharathi Institute of Technology (VBIT),
Ghatkesar, Hyderabad, India

² Jawaharlal Nehru Technological University Hyderabad (JNTUH),
Hyderabad, India

oscillation (ENSO) (Gurubaran et al. 2005) which in turn could affect the stratospheric interannual oscillation (SIO) (Chen et al. 2003). The causes of tidal variabilities have been extensively studied but still it remains an open question. Reports of tidal oscillations and their variabilities are quite sparse in the lower atmosphere particularly over tropical sites (Sasi et al. 1998; Dutta et al. 2002; Seidel et al. 2005; Alexander and Tsuda 2008). The coupling between troposphere and stratosphere has been reported to be associated with the atmospheric variability (Ambaum and Hoskins 2002). It has been observed that a small variation in solar ultraviolet flux is reflected in stratospheric temperature which affects the troposphere through dynamical and radiative coupling (McCormack and Hood 1996; Kodera and Kuroda 2002). Studies on long-term variability of solar tides and their dependence on 11-year solar cycle, particularly in the stratosphere and troposphere, their source regions, are rudimentary mainly because of nonavailability of observational data.

This paper presents climatology of diurnal tide and its long-term variabilities in the lower atmosphere over a tropical Indian station based on European Centre for Medium-Range Weather Forecasts (ECMWF) reanalysis data of 22 years. MST radar data of Gadanki for 1 year (May 2005–April 2006) is also used for comparison of tidal parameters. The details of data, overview of Global Scale Wave Model (GSWM), and the method of analysis are presented in Section 2. Section 3 describes the background wind and its seasonal behavior. Amplitudes and phases of diurnal tides have been discussed in Section 4. Section 5 describes the long-term variabilities of diurnal oscillation. Finally, the summary of the paper is presented in Section 6.

2 Data and method of analysis

The ECMWF reanalysis (ERA–interim) datasets are potentially useful to carry out climatological studies in the troposphere and stratosphere since the data is available globally for various atmospheric parameters with a good spatial resolution ($1.5^\circ \times 1.5^\circ$). Sakazaki et al. (2012) used six different reanalysis datasets to investigate diurnal temperature tide in the lower and middle atmosphere and observed that the ERA–interim data could reproduce realistic diurnal tides. The 6-hourly sampling rate of ERA–interim data is also sufficient to obtain reliable estimates of diurnal tides (McCormack et al. 2010). We analyze 22 years (January 1991 to December 2012) ERA–interim data of winds to study the characteristics and long-term variabilities of diurnal tides for a tropical station (13.5° N, 79.5° E) in the northern hemisphere. Wind data has been downloaded from the site <http://www.data-portal.ecmwf.int/data/d/interim-daily/leveltype=pl>.

The diurnal cycle common mode hourly observations of wind measured by Indian MST radar (13.5° N, 79.2° E)

between 4 and 20 km from May 2005 to April 2006 have been used to delineate amplitudes and phases of 24-h oscillation. The radar-measured winds are initially inspected visually for outliers. Wind profiles are then averaged for three consecutive hours, and standard deviations (σ) are calculated. Outliers are removed by taking these mean winds at each height and discarding values exceeding 1.7 times the standard deviation. Points going beyond this limit are treated as outliers and removed. Data gaps are filled with linear interpolation. Quality of the data is found to be quite good and such interpolations are rare.

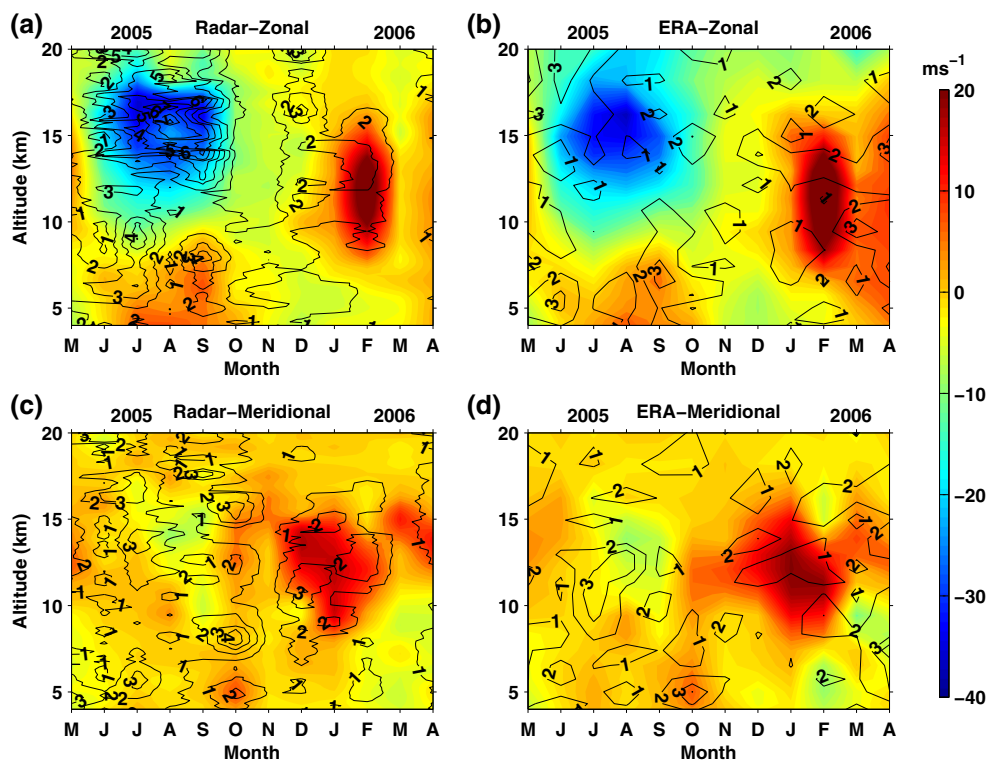
Figure 1 illustrates the comparison between radar-measured winds and simultaneous ERA winds in contour forms. A fair agreement can be observed except at a few heights which are quite reasonable since only single day's data of each month are compared. Close proximity between the ground-based measurements (radar and radiosonde) and ERA–interim datasets has been reported from the same site earlier (Ratnam et al. 2014 and references therein). Radar-measured winds show some perturbations with short vertical wavelengths (~ 1 km) particularly in the lower stratosphere for the meridional component between June and October which appear to be due to some enhanced wave activity or turbulence. Such fluctuations are a common feature during southwest monsoon season which can be observed by high-resolution (150 m) radar measurements (Dhaka et al. 2014; Dutta et al. 2009; Tsuda et al. 2004). The horizontal winds are used to extract the tidal components. Note that considering the time resolution of the reanalysis data, we confined to diurnal tides, only. The analysis procedure is discussed later in this section.

In order to verify the estimated tidal variabilities, we used GSWM-09 tides (details mentioned in Section 2.1). In addition, effect of outgoing longwave radiation (OLR) on diurnal tides has been studied using OLR data from National Center for Environmental Prediction (NCEP)/National Center for Atmospheric Research (NCAR). Ozone mixing ratio and water vapor have been obtained from the same ERA–interim site to investigate the causes of seasonal variability of diurnal oscillation.

2.1 GSWM overview

The GSWM is a two-dimensional numerical model that solves the linearized tidal equation (Hagan et al. 1995). The linear approximation is sufficient for the computation of the wave response to any given forcing. In a tutorial, Forbes (1995) stressed the need of addressing nonmigrating longitude-dependent diurnal tide in the theoretical and numerical models. Subsequently, several investigations have been reported highlighting the importance of nonmigrating tide forced by the latent heat release of precipitating clouds (Williams and Avery 1996; Hagan and Forbes 2002). These

Fig. 1 Contours of zonal and meridional winds of Gadanki MST radar (a, c) and simultaneous ERA winds (b, d), respectively, between May 2005 and April 2006. Line contours of errors have been plotted in *black color*



lower atmospheric waves excited by the absorption of infrared radiation and latent heat release propagate upwards to the MLT region along with the migrating component. The eastward propagating zonal wave number 3 component (DE3) is reported to dominate near 115 km during most of the year (Hagan et al. 2007). The GSWM model includes all important processes of global atmospheric tidal response but does not take into account the excitation of some tidal oscillations by wave–wave interaction. Zhang et al. (2010a) reported that the radiative heating in the troposphere without considering the latent heating can account for a considerable portion of the longitudinal variability due to nonmigrating tides. The authors ran the same GSWM model with total (latent + radiative) heating and improved, more realistic background winds and temperature (Zhang et al. 2010b) which culminated into GSWM-09. The GSWM-09 also incorporates all migrating and nonmigrating diurnal and semi-diurnal components.

2.2 Analysis of diurnal amplitude and phase

Zonal and meridional wind velocities of 22 years (January 1991 to December 2012) have been used to carry out composite tidal analyses to study the characteristics of amplitudes and phases of diurnal tides. Time series of zonal and meridional wind data for 10 days (first to tenth) of January 1991 are used to form 10-day composite and are subjected to harmonic analysis with least square fitting considering the prevailing wind and the diurnal component. Each wind component can

be represented by a function of time in the expression.

$$A(t) = A_0 + A_{24} \cos\left(\frac{2\pi t}{24} + \phi_{24}\right) \quad (1)$$

where A_0 is the prevailing wind and A_{24} and ϕ_{24} are the amplitude and phase of diurnal tide. Since there are four data points with a gap of 6 h on each day, it is not possible to resolve semi-diurnal and ter-diurnal components. The results of this 10-day composite are assigned to 5 January 1991. The 10-day window is then continuously shifted by 1 day, and similar analysis is carried out till the end of December 2012. The results of last window, i.e., 22 to 31 December 2012 is assigned to 26 December 2012. This gives rise to the time windows that are equal to the number of days of the month for different months, except for the first (27 windows for January 1991) and last (26 windows for December 2012) months. The mean of the amplitude profiles obtained in these sets is considered to be the monthly mean amplitude–height profiles for 22 years yielding 22 profiles of each month (January to December). The average of these 22 profiles is accepted as the mean profile of the particular month.

The altitude profiles of phases are obtained differently. The distribution of phase values is found to be very broad which makes the average meaningless. Moreover, overlapping of phase peaks while averaging may distort the phase information. The phase data are converted into discreet sets by binning them into 1-h bins (Seidel et al. 2005), and the modal values of these profiles is accepted as the height variation of diurnal

phase for that particular month. Similar exercise is carried out for 22 years yielding 22 phase profiles for each month. The modes of these 22 modal profiles of each month are then considered to be the phase profile for that particular month. As an example, all the zonal phase altitude profiles for the month of December over 22 years have been plotted in contoured frequency with altitude form which is shown in the left panel of Fig. 2. The right panel depicts a comparison between mode of modes and mean of means for the same month along with corresponding GSWM-09 values. It is clear from these diagrams that the mode of modes picks up the correct trend of the phase profile.

3 Background wind (ERA) and its seasonal behavior

A brief description of the background wind is presented since it plays a vital role in the propagation of tidal oscillation. The monthly wind profiles are averaged over 22 years and are depicted in Fig. 3a–l with corresponding standard deviations. Zonal winds are generally found to be westward and weak below ~ 7 km between November and April which change to weak eastward wind during summer months. The upper tropospheric winds are found to be eastward during winter and slowly change over to westward winds with the advance of summer months. Strong westward jets ($\sim -35 \text{ ms}^{-1}$) are observed in the months of June–July–August below the tropopause with large vertical shear in horizontal wind. Stratospheric winds are also found to be westward during summer months. The strength of westward winds slowly reduces in the fall equinox months and later they change over to

weak eastward winds above 30 km in winter. Meridional winds are generally weakly northward between 8 and 18 km during winter and spring equinox. Northward jets are seen at ~ 12 km between October and April with maximum velocities in December ($\sim 8\text{--}9 \text{ ms}^{-1}$). Northward winds change to weak southward winds during summer in the same altitude region. Stratospheric winds are very weak and almost close to zero. The pattern of ERA winds described here agrees quite well with the climatology of wind system measured by Gadanki MST radar (Narendra Babu et al. 2008). The variabilities of wind velocities as depicted by the standard deviations are larger at stratospheric heights compared to those in the troposphere. The error bars vary between 0.05 and 1.3 ms^{-1} in the troposphere and almost get doubled at stratospheric heights.

4 Amplitudes and phases of diurnal tides

The diurnal cycle (24 points) wind data measured by Gadanki radar and simultaneous ERA data (4 points) of the same days between May 2005 and April 2006 as mentioned in Section 2 have been subjected to harmonic analysis. Comparisons of the amplitudes and phases obtained from the analyses of 1-year data (both MST radar and ERA data) are illustrated in Fig. 4a–l and Fig. 5a–l, respectively. Higher order polynomials have been fitted to the radar measured amplitude and phase profiles to obtain smooth variations. The measured amplitudes are quite large compared to those derived using ERA winds in most of the months indicating that the diurnal wind might have been underestimated in reanalysis data. Agreements of

Fig. 2 **a** Contour frequency altitude diagram of diurnal phases for the month of December. **b** Comparison of mean of means and mode of modes of diurnal phase along with GSWM-09 values for December

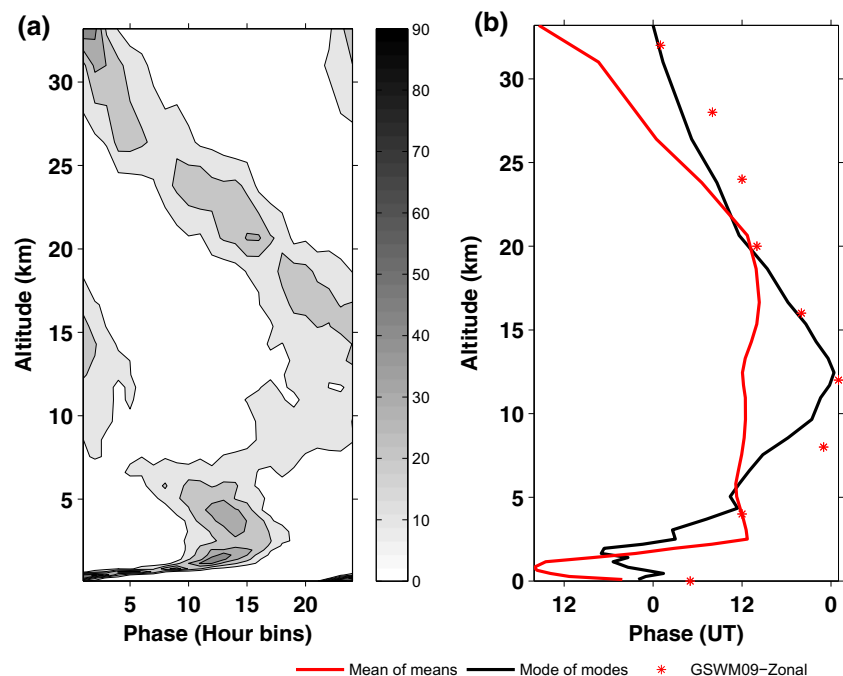
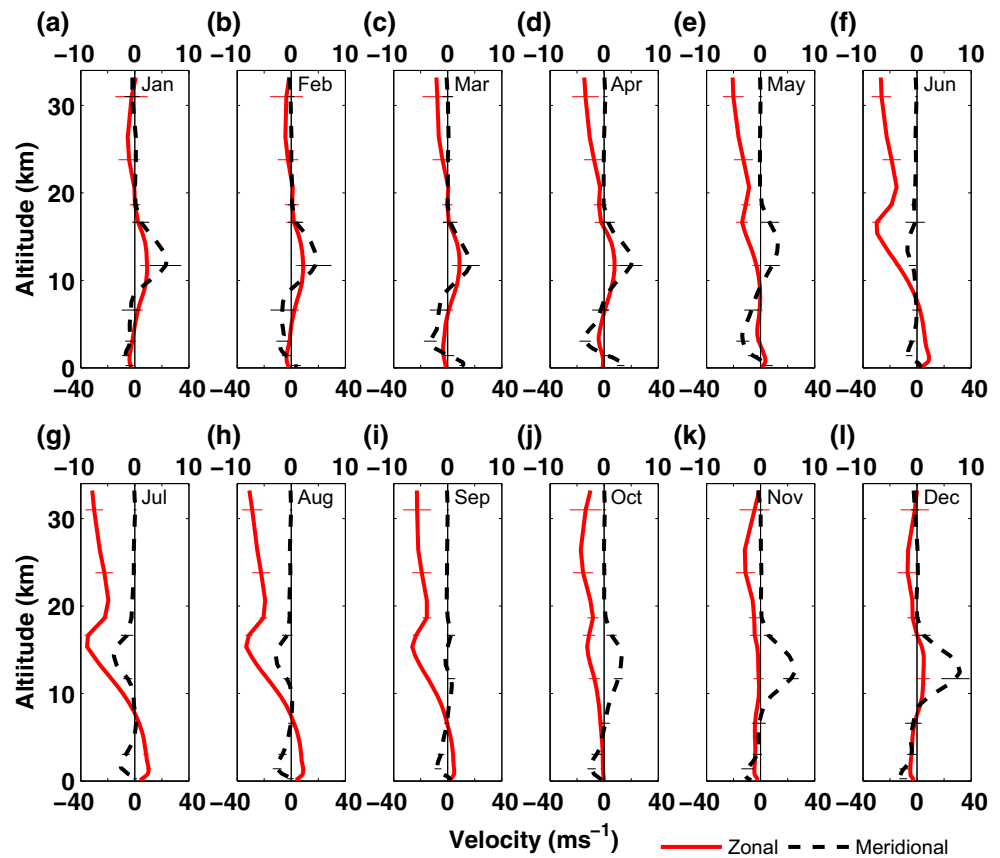


Fig. 3 a–l Mean monthly wind profiles of 22 years (ERA data) with standard deviations at a few heights. Zonal and meridional components are shown with *bottom* and *top* abscissa, respectively



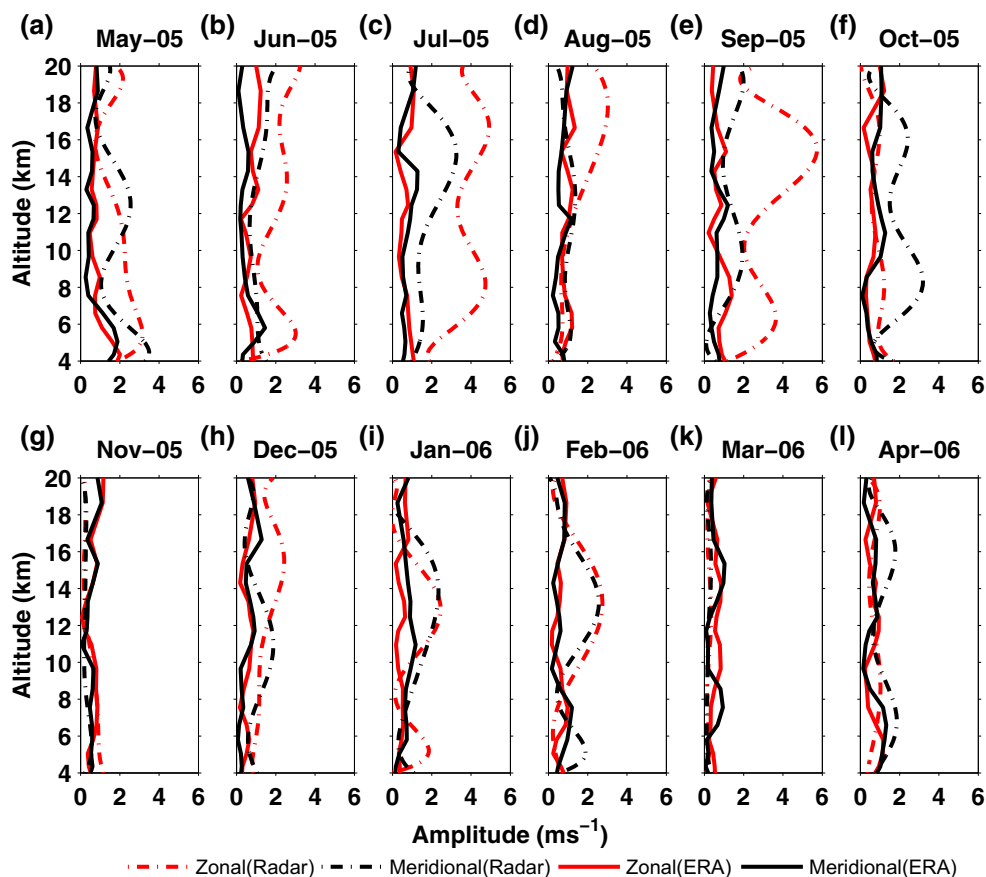
phase profiles are quite satisfactory except for August, November, December, and April.

Mean diurnal amplitude profiles of each month averaged over 22 years (ERA) are shown as filled contours in Fig. 6a, b for both the wind components along with line contours of standard deviations. Contours of GSWM-09 values have also been plotted in Fig. 6c, d for comparison. Model amplitudes compare fairly well with the computed values for both the wind components in the troposphere except below 5 km where large differences between the two are observed. The discrepancy is found to be maximum around 1.5 km where large amplitudes are observed between March and September. The computed amplitudes show differences with the model values in spite of incorporating total heating and more realistic winds in GSWM-09. Sakazaki et al. (2012) has compared GSWM-09 data with SABER and reanalysis for westward propagating wave number 1 diurnal migrating component (DW1). They report reasonable agreement in the basic features and seasonal variation but the antisymmetric structure in the tropics are found to be weak in GSWM.

Diurnal amplitudes obtained for zonal and meridional winds in the present work show peak values ($\sim 2.7 \pm 0.5$ and $2 \pm 0.5 \text{ ms}^{-1}$) below 5 km which are more prominent during summer months particularly for the zonal component. This could be due to the nonmigrating tides generated weakly by

diurnally varying planetary boundary layer heat flux and high level of water vapor. Moreover, the background zonal wind in the region is eastward which does not affect the westward propagating migrating tide. The temperature diurnal oscillations reported by Seidel et al. (2005) also show large amplitudes near surface and at 850 hPa. Similar observations were made by Wallace and Patton (1970). Diurnal amplitudes are also found to be appreciable in the mid-stratosphere ($\sim 2 \pm 0.3 \text{ ms}^{-1}$) during fall equinox and early winter for the zonal component whereas the meridional component shows larger values between October and April. The background zonal wind in this region slowly changes its direction. Larger variabilities can be observed at stratospheric heights above 25 km as depicted by the error contours. Amplitudes reported using MST radar measurements for this latitude in the upper troposphere and lower stratosphere range approximately between 2 and 2.5 ms^{-1} (Sasi et al. 1998; Dutta et al. 2002). The diurnal amplitude reported by Tsuda et al. (1997) for Indonesia using radiosonde measurement in the troposphere is $\sim 1 \text{ ms}^{-1}$ which gets reduced in the lower stratosphere. Their amplitudes agreed better with the model values of Ekanayake et al. (1997) which accounted for nonmigrating tides. The zonal wind amplitudes observed at Koto Tabang (Indonesia) exceeded 2 ms^{-1} at 16–17 and 24–26 km where the zonal wind shear was greater than $15 \text{ ms}^{-1} \text{ km}^{-1}$ (Alexander and Tsuda 2008). The tidal amplitude estimated using radar data

Fig. 4 a–l Comparisons of measured diurnal amplitudes with those derived from ERA winds between May 2005 and April 2006



in the troposphere and lower stratosphere for Jicamarca (12° S) is $\sim 1 \text{ ms}^{-1}$ (Riggin et al. 2002). Sasi and Krishnamurthy (1990) studied tidal oscillations using rocket data of a tropical station Balasore (21.5° N). They reported the amplitude of diurnal tides to be $\sim 2 \text{ ms}^{-1}$ for both the components up to 40 km above which it increased.

The monthly phase profiles obtained as described in Section 2.2 are smoothed by taking 5-point running mean and are displayed in Fig. 7 for both the wind components along with the GSWM-09 values for 12° N latitude and 80° E longitude which is one of the closest to the site under consideration. Using the modes of the monthly modal profiles instead of the means reduces the phase errors considerably without any loss in its characteristic features. The differences between zonal and meridional phases vary approximately between 4 and 6 h. Good agreement can be observed between the derived and GSWM model phases. Downward phase propagation can be seen above 15–20 km. Small altitude regions just before the points of inflection show constant phases and might be the source regions of tidal oscillations (Williams and Avery 1996; Sasi et al. 1998; Kumar, 2006). Vertical wavelength of diurnal oscillation has been calculated using phase profiles in the lower stratosphere

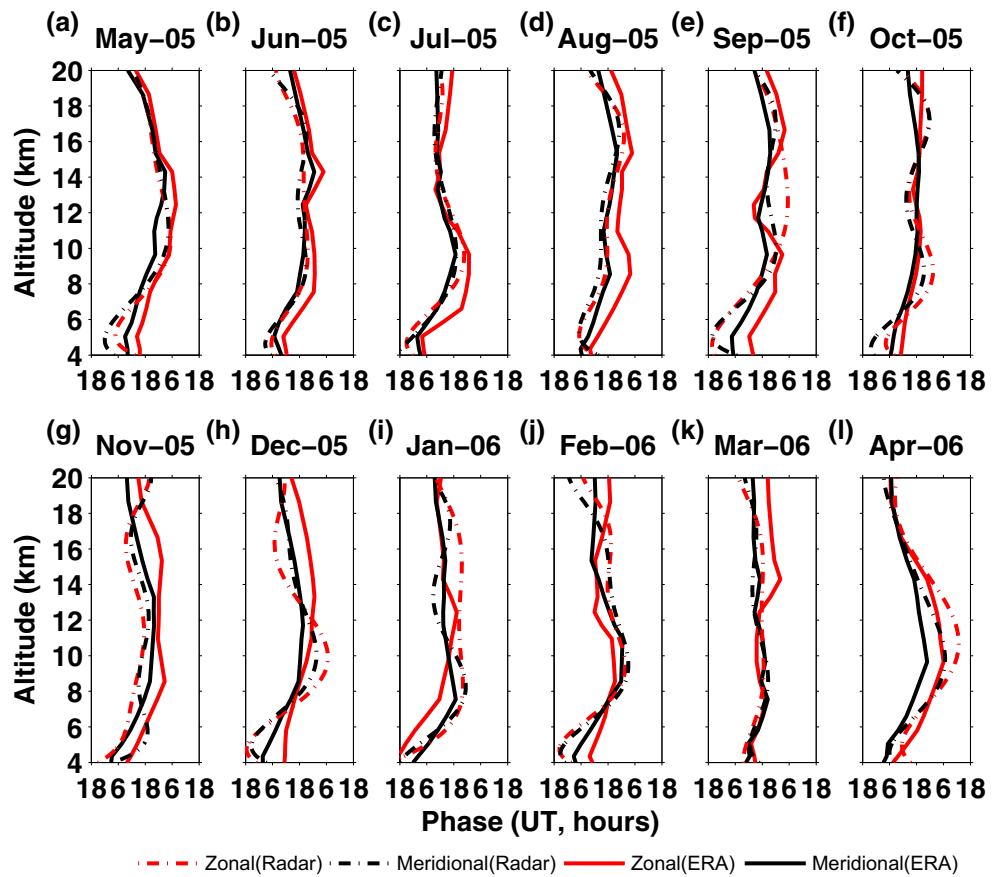
and is found to vary between ~ 20 and 30 km which indicates a superposition of migrating and nonmigrating tides.

5 Variabilities of diurnal tidal amplitudes

5.1 Seasonal variations

The mean diurnal amplitudes of each month from January to December are shown in Fig. 6a, b. Large amplitudes are seen in the lower troposphere below $\sim 5 \text{ km}$ mostly during summer months when the background zonal winds are eastward. This lower tropospheric region contains most of the water vapor and convection is present in this season which triggers localized nonmigrating tides (see Section 2). Sakazaki et al. (2015) also suggested that diabatic heating in the troposphere plays a significant role in the seasonal variation of nonmigrating tides. Zonal diurnal amplitudes are observed to get reduced between ~ 8 and 15 km particularly during summer months when the background westward wind is quite strong in the region which filters out the westward propagating migrating component. The amplitude picks up again and maximizes between 25 and 30 km mostly during equinoxes and

Fig. 5 a–l Same as Fig. 4 but for phases



winter when the zonal wind becomes less westward or weakly eastward. The seasonal variability of 24-h tide appears to have similar trends for both zonal and

meridional components. Maximum meridional amplitudes are observed in the lower troposphere and near the surface during summer months. Diurnal amplitudes decrease in

Fig. 6 Contours of diurnal amplitudes for zonal and meridional components of ERA data (a, b) and GSWM-09 (c, d). Error contours are plotted over ERA amplitudes with white lines

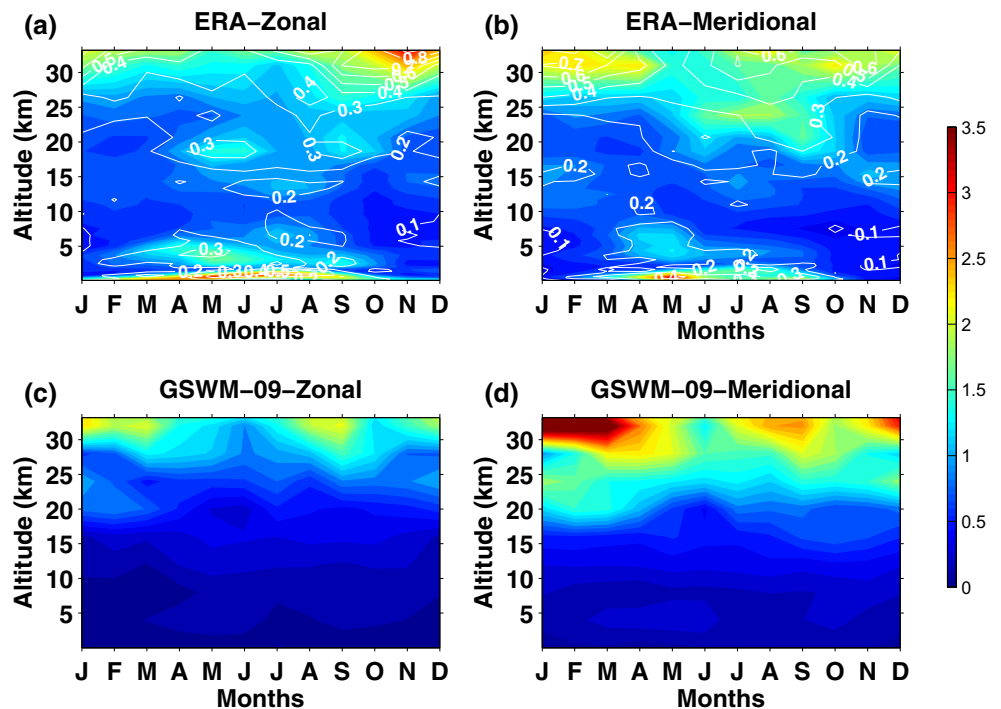
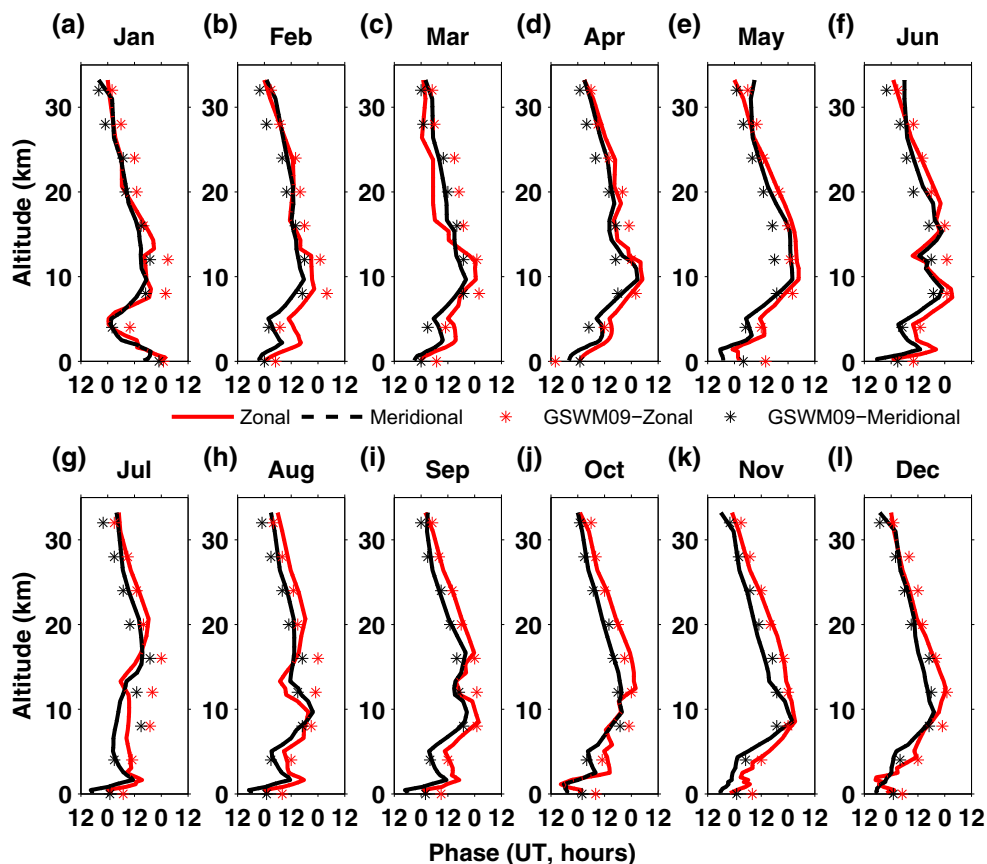


Fig. 7 a–l Height variations of zonal and meridional diurnal phases. GSWM-09 phases have been plotted for comparison



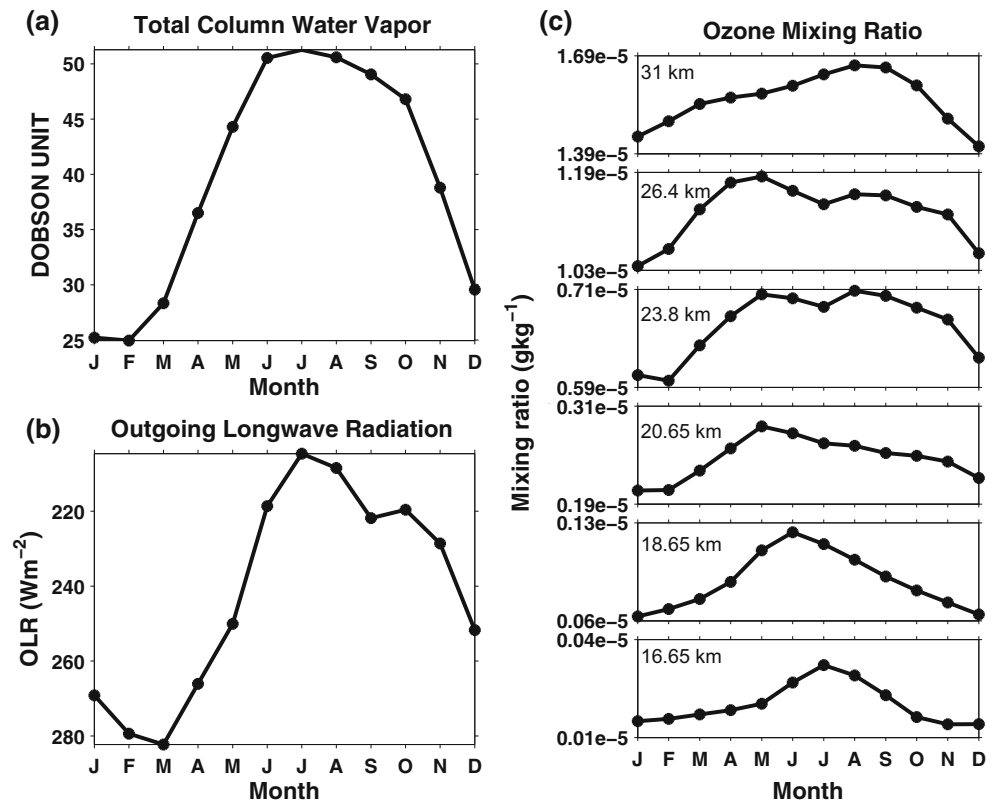
the upper troposphere which again attains appreciable values at stratospheric heights during equinoxes and winter. It should be remembered that north–east monsoon prevails in this region during fall equinox and early winter when the surrounding area becomes convective.

The influence of water vapor, OLR, and ozone on the seasonal variation of diurnal amplitudes has been investigated by correlation studies. Water vapor is recognized to be very important component which forces diurnal tide, and the maximum of its heating rate is supposed to be near 8 km (Chapman and Lindzen 1970). Seasonal variations of total column water vapor (Fig. 8a) show maximum value during the wet season (June–July–August) when south–west monsoon is vigorous over this region. Correlation study carried out between diurnal amplitude and water vapor reveals maximum values of the correlation coefficient to be ~ 0.59 and ~ 0.52 for zonal and meridional winds, respectively. Larger tidal amplitudes are observed in the troposphere during convective season. The level of convection can be represented by OLR. Lower values of OLR means deeper/higher convection in the tropical region. The average seasonal variation of OLR over 22 years (Fig. 8b) is found to have two peaks in summer and fall equinox. The second peak is smaller compared to the first peak. The correlation coefficients between amplitudes of diurnal

oscillation and OLR are -0.34 and -0.24 for zonal and meridional components, respectively.

Ozone radiative heating is also an important source of diurnal tide in the stratosphere. Seasonal variation of ozone mixing ratio for a few heights in troposphere and stratosphere is depicted in Fig. 8c. The variation is found to be basically a mixture of annual and semi-annual oscillation. The annual oscillation is found to be prominent at tropospheric heights whereas the semi-annual variation becomes prominent in stratosphere where ozone mixing ratio has significant values. A correlation study between monthly ozone mixing ratio and corresponding diurnal amplitude over 22 years yields significant correlation ($\rho \approx 0.66$ and $\rho \approx 0.60$ for zonal and meridional components, respectively). All the correlation coefficients obtained in this study are with 95 % confidence levels. The seasonal variation of diurnal oscillation appears to be closely linked with ozone variation in the mid-stratosphere. The diurnal temperature tide shows an annual variation peaking in the summer in northern hemisphere at ~ 33 km (Wu and Jiang 2005). Seidel et al. (2005) finds the diurnal cycle amplitudes to be larger over land than ocean and generally larger in summer than in winter. The difference between land and sea was not prominent in upper troposphere and stratosphere. As an exception in the tropics, they observed the seasonal cycle for

Fig. 8 **a** Mean seasonal variation of total column water vapor. **b** Mean seasonal variation of outgoing longwave radiation (OLR). **c** Mean seasonal variation of ozone mixing ratio for a few stratospheric heights



diurnal tide below 850 hPa to be maximum in the period from November to May.

5.2 Annual and interannual variations

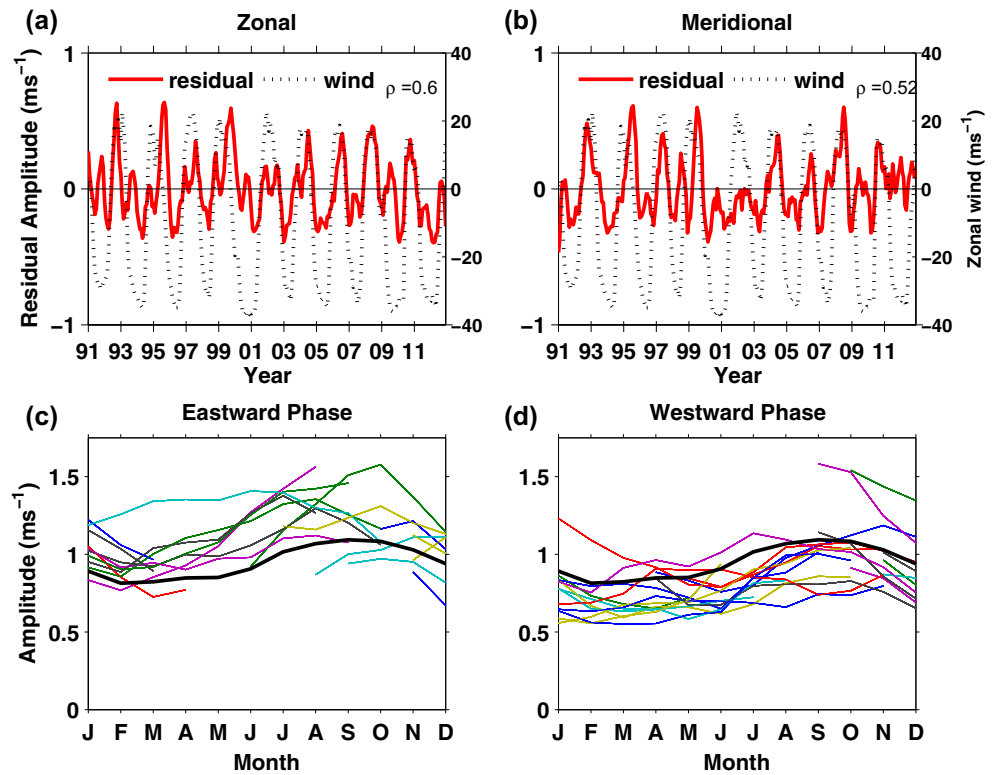
Diurnal tide is known to display strong interannual variability in the MLT and stratospheric regions (Burrage et al. 1995; Vincent et al. 1998; Wu and Jiang 2005). Causes of this variability could be the variations in mean zonal wind including QBO. The diurnal oscillation in the MLT region over Adelaide (35° S) in the southern hemisphere has been linked to QBO in the equatorial stratosphere where the amplitude maximizes during March equinox (Vincent et al. 1998). The diurnal amplitudes obtained in the present study over 22 years have been examined to observe such variability. The time variations of monthly tidal amplitudes are smoothed by taking a 3-point running mean for clarity which show annual variation in the lower troposphere whereas the variability slowly turns into a mixture of annual and biennial oscillations at stratospheric heights (figure not shown). Annual oscillation (AO) dominates below the tropopause, and QBO is found to play an important role at stratospheric heights along with AO.

The influence of QBO wind on tidal amplitudes has been investigated by forming the time series of residuals obtained after subtracting the 22 years' mean from individual monthly amplitude. These residuals have been plotted with corresponding equatorial zonal wind for both the components at

the height of maximum QBO (~26 km). The in-phase relationship between tidal amplitudes and the QBO winds at ~26 km can be clearly seen with reasonably high values of correlation coefficients (0.6 for zonal and 0.52 for meridional components) and are shown in Fig. 9a, b. To test the relationship further, the 24-h amplitude data of each year has been grouped into eastward and westward according to the QBO phase. Time series of diurnal tides (monthly averages) for zonal component are illustrated in Fig. 9c, d for eastward and westward phases of QBO. Note that the thick lines represent mean values of 22 years. It can be observed that the diurnal amplitudes peak between October and December and show larger values than the mean during eastward phase of QBO whereas the amplitudes are less compared to the mean during the westward phase. AO is also found to be appreciable at these stratospheric heights. Larger interannual variability has been reported for Kauai in the northern hemisphere during October–November in the MLT region (Fritts and Isler 1994).

In a recent paper, Kishore Kumar et al. (2014b) reported different criteria to select Stratospheric Quasi Biennial Oscillation (SQBO). We have followed their “strongest wind approach” to correlate the strongest zonal wind at equator between 16 and 32 km with the diurnal tidal amplitudes over Gadanki in the same altitude region. The correlation coefficient is found to be maximum at ~26 km ($\rho = 0.4$) and is poor at other altitudes. This method does not appear to be a better alternative in the stratospheric region.

Fig. 9 **a** Time series of zonal residuals along with equatorial QBO winds at ~26 km. **b** Same as **a** but for meridional residuals. **c** Plots of the amplitude of zonal diurnal tide at ~26 km for years when the zonal mean QBO is in eastward phase. **d** Same as **c** but when the zonal mean QBO is in westward phase

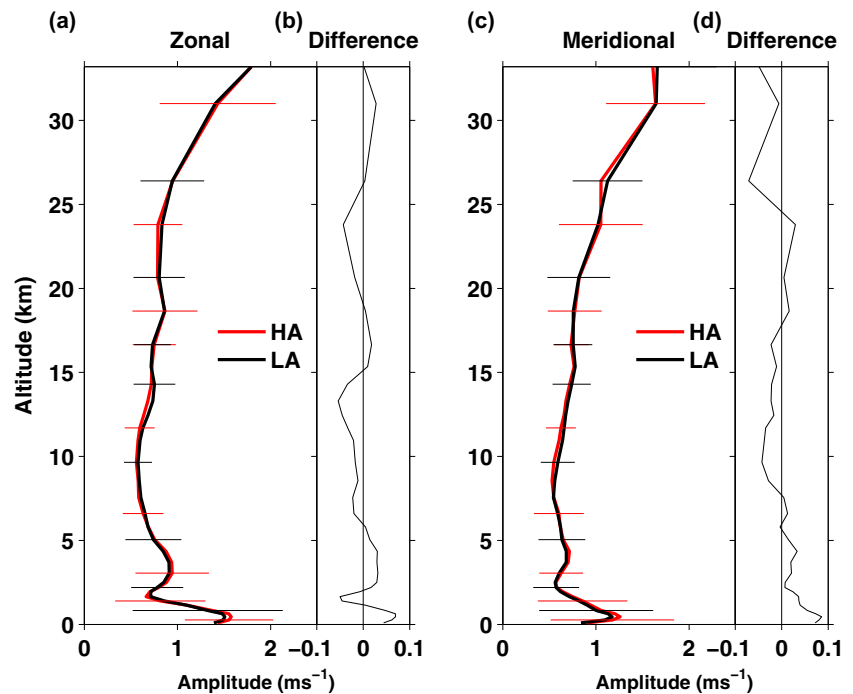


5.3 Solar activity variations

Investigation of the long-term solar activity variations of tidal amplitudes has been carried out by separating the amplitudes of 22 years into two phases of the solar cycles. The solar maxima and minima years are split based on whether the solar

$F_{10.7}$ cm fluxes of the corresponding years are above or below the mean value (Ogi et al. 2003). Thus, 9 years (1991, 1992, 1998–2003, 2012) are designated as high activity (HA) years and the rest 13 years (1993–1997, 2004–2011) as low activity (LA) years. The amplitude height profiles of diurnal tide are averaged for solar HA and LA years separately and are

Fig. 10 Mean profiles of solar HA and LA diurnal amplitudes (**a**, **c**) with corresponding standard deviations at a few heights for both the wind components. The difference profiles are shown in **b** and **d**



illustrated in Fig. 10a–d for both the components along with the difference profiles. The difference profiles show very low values ($\pm 0.05 \text{ ms}^{-1}$) which are within the limits of uncertainties and cannot be attributed to solar activity variations. Recent analysis by Ratnam et al. (2014) shows larger tidal amplitudes at stratospheric heights in the extended period of solar cycle minimum though, in general, they did not notice any correlation between the two.

6 Summary

The characteristics of diurnal tides have been delineated using diurnal cycle (24 h) winds measured by Gadanki MST radar for one year. The derived amplitudes and phases have been compared with the results of simultaneous ERA–interim data. Measured amplitudes show larger values whereas phase agreements are quite good. It should be noted that the diurnal amplitudes and phases obtained here using radar and ERA winds belong to a single location and correspond to superposition of all migrating and nonmigrating components.

The climatology of 24-h tidal oscillations presented in this study has been estimated using ERA–interim winds for two solar cycles (1991–2012). The wind data have been analyzed to extract monthly diurnal tidal components up to an altitude of ~ 33 km. Mean diurnal amplitudes and phases for different months are compared with GSWM-09 which takes into account both the migrating and nonmigrating components. A reasonably good agreement is observed between the computed and model values above ~ 5 km. It appears that the nonmigrating diurnal component is still underestimated in GSWM-09 at least for the tropics. Maximum tidal amplitudes obtained in the present study at ~ 1.5 km are $\sim 2.7 \pm 0.5$ and $\sim 2 \pm 0.5 \text{ ms}^{-1}$ for zonal and meridional components, respectively. Amplitudes get reduced between 8 and ~ 20 km where background zonal wind is strongly westward which filters out the dominant migrating tidal component. Amplitudes start increasing again above 20 km with a simultaneous change in wind direction and attain maximum amplitude ($\sim 2 \pm 0.35 \text{ ms}^{-1}$) in the mid-stratosphere.

Long-term tidal variabilities have been investigated and an attempt has been made to find their causes. Large diurnal amplitudes are observed in the lower troposphere below ~ 5 km which are more prominent during summer months and equinoxes when the corresponding background winds are weakly eastward and nonmigrating tides are present. This trend of tidal amplitude is possibly linked to the total column water vapor and OLR in the tropospheric region. Even the ozone mixing ratio shows an annual variation in the troposphere. This ratio slowly becomes semi-annual in stratospheric region with a stronger peak in fall equinox and the seasonal variation of diurnal amplitude follows this trend. Forcing due to water vapor, convection and ozone seems to be

important for shaping the seasonal variability of diurnal tides. The interannual variability observed in the stratosphere can be directly linked to the SQBO. Solar activity does not appear to have significant effect on diurnal tides.

Future study will concentrate on latitudinal and longitudinal variations of diurnal oscillations. The results presented here should be taken with a little caution since the temporal resolution of the data is just adequate for resolving diurnal tide.

Acknowledgments ERA–interim data were provided by the European Centre for Medium-Range Weather Forecasts (ECMWF) through their web site. Two of the authors, P. Vinay Kumar and Salauddin Mohammad, are thankful for the research fellowship offered by Indian Space Research Organization (ISRO) under its Climate And Weather of Sun–Earth System (CAWSES–II) program. We acknowledge Dr. B. Bapiraju and Dr. P.V. Rao for their kind suggestions. Authors are grateful to anonymous reviewers for their constructive comments. The authors also thank the college management for their kind encouragement.

References

- Alexander SP, Tsuda T (2008) Observations of the diurnal tide during seven intensive radiosonde campaigns in Australia and Indonesia. *J Geophys Res* 113:D04109. doi:10.1029/2007JD008717
- Ambaum MHP, Hoskins BJ (2002) The NAO troposphere–stratosphere connection. *J Clim* 15:1969–1978
- Burrage MD, Hagan ME, Skinner WR, Wu DL, Hays PB (1995) Long-term variability in the solar diurnal tide observed by HRDI and simulated by the GSWM. *Geophys Res Letts* 22(19):2641–2644. doi:10.1029/95GL02635
- Chang LC, Palo SE, Liu HL (2011) Short-term variability in the migrating diurnal tide caused by interactions with the quasi 2 day wave. *J Geophys Res* 116:D12112. doi:10.1029/2010JD014996
- Chapman S, Lindzen RS (1970) Atmospheric tides. Springer, New York
- Chen W, Takahashi M, Graf H–F (2003) Interannual variations of stationary planetary wave activity in the northern winter troposphere and stratosphere and their relations to NAM and SST. *J Geophys Res* 108(D24):4797. doi:10.1029/2003JD003834
- Dhaka SK, Malik V, Shibagaki Y, Hashiguchi H, Fukao S, Shimomai T, Chun H–Y, Takahashi M (2014) Comparison of vertical wavelengths of gravity waves emitted by convection in the UTLS region at Koto Tabang (0.20°S, 100.32°E) and Gadanki (13.5°N, 79.2°E) using radars. *Indian J Radio Space Phys* 43(1):24–40
- Dutta G, Ajay Kumar MC, Vinay Kumar P, Ratnam MV, Chandrashekar M, Shibagaki Y, Mohammad S, and Basha HA (2009) Characteristics of high-frequency gravity waves generated by tropical deep convection: case studies. *J Geophys Res* 114(D18109), doi: 10.1029/2008JD011332.
- Dutta G, Bapiraju B, Balasubrahmanyam P, Siddiqui MAA, Basha HA (2002) Seasonal variation of solar tides in the troposphere and lower stratosphere over Gadanki: comparisons with the global scale wave model. *Radio Sci* 37(2), doi: 10.1029/2000RS002571.
- Ekanayake EMP, Aso T, Miyahara S (1997) Background wind effect on propagation of nonmigrating diurnal tides in the middle atmosphere. *J Atmos Solar Terr Phys* 59:401–429
- Forbes JM (1995) Tidal and planetary waves, in the upper mesosphere and lower thermosphere: a review of experiment and theory. *Geophys Monogr Ser* 87:67–87

- Fritts DC, Isler JR (1994) Mean motions and tidal and two-day structure and variability in the mesosphere and lower thermosphere over Hawaii. *J Atmos Sci* 51:2145–2164
- Fritts DC, Vincent RA (1987) Mesospheric momentum flux studies at Adelaide, Australia: observations and a gravity wave–tidal interaction model. *J Atmos Sci* 44:605–619
- Gurubaran S, Rajaram R, Nakamura T, Tsuda T (2005) Interannual variability of diurnal tide in the tropical mesopause region: a signature of the El Niño–Southern Oscillation (ENSO). *Geophys Res Lett* 32: L13805. doi:10.1029/2005GL022928
- Hagan ME, Forbes JM, Vial F (1995) On modeling migrating solar tides. *Geophys Res Lett* 22:893–896
- Hagan ME, Forbes JM (2002) Migrating and nonmigrating diurnal tides in the middle and upper atmosphere excited by tropospheric latent heat release. *J Geophys Res* 107(D24):4754. doi:10.1029/2001JD001236
- Hagan ME, Maute A, Roble RG, Richmond AD, Immel TJ, England SL (2007) Connections between deep tropical clouds and the Earth's ionosphere. *Geophys Res Lett* 34:L20109. doi:10.1029/2007GL030142
- Hall GE, Nambrothiri SP, Manson AH, Meek CE (1995) Daily tidal, planetary wave and gravity wave amplitudes over the Canadian Prairies. *J Atmos Terr Phys* 57:1553–1567
- Hocking WK, Hocking A (2002) Temperature tides determined with meteor radar. *Ann Geophys* 20:1447–1467
- Kishore Kumar G, Singer W, Oberheide J, Grieger N, Batista PP, Riggan DM, Clemesha BR (2014a) Diurnal tides at low latitudes: radar, satellite, and model results. *J Atmos Solar Terr Phys* 118:96–105. doi: 10.1016/j.jastp.2013.07.005.
- Kishore Kumar G, Kumar KK, Singer W, Züllicke C, Gurubaran S, Baumgarten G, Ramkumar G, Sathishkumar S, Rapp M (2014b) Mesosphere and lower thermosphere zonal wind variations over low latitudes: relations to local stratospheric zonal winds and global circulation anomalies. *J. Geophys. Res. Atmos.* 119, 5913 – 5927. doi:10.1002/2014JD021610.
- Kodera K, Kuroda Y (2002) Dynamical response to the solar cycle. *J Geophys Res* 107(D24):4749. doi:10.1029/2002JD002224
- Kumar KK (2006) VHF radar observations of convectively generated gravity waves: some new insights. *Geophys Res Lett* 33:L01815. doi:10.1029/2005GL024109
- McCormack JP, Hood LL (1996) Apparent solar cycle variations of upper stratospheric ozone and temperature: latitude and seasonal dependencies. *J Geophys Res* 101:20933–20944
- McCormack JP, Eckermann SD, Hoppel KW, Vincent RA (2010) Amplification of the quasi-two day wave through nonlinear interaction with the migrating diurnal tide. *Geophys Res Lett* 37:L16810. doi:10.1029/2010GL043906
- Meek CE, Manson AH, Drummond JR (2011) Test of diurnal and semi-diurnal tidal analysis of temperatures from SABER-like sampling of a realistic global model, CMAM–DAS. *Ann Geophys* 29:723–730. doi:10.5194/angeo-29-723-2011
- Narendra Babu A, Kumar KK, Kishore Kumar G, Ratnam MV, Rao SVB, Rao DN (2008) Long-term MST radar observations of vertical wave number spectra of gravity waves in the tropical troposphere over Gadanki (13.5° N, 79.2° E): comparison with model spectra. *Ann Geophys* 26:1671–1680. doi:10.5194/angeo-26-1671-2008
- Ogi M, Yamazaki K, Tachibana Y (2003) Solar cycle modulation of the seasonal linkage of the North Atlantic Oscillation (NAO). *Geophys Res Lett* 30(22):2170. doi:10.1029/2003GL018545
- Ratnam MV, Rao NV, Vedavathi C, Krishnamurthy BV, Rao SVB (2014) Diurnal tide in the low-latitude troposphere and stratosphere: long-term trends and role of the extended solar minimum. *J Atmos Sol Terr Phys* 121:168–176
- Riggan DM, Kudeki E, Feng Z, Sarango MF, Lieberman RS (2002) Jicamarca radar observations of the diurnal and semidiurnal tide in the troposphere and lower stratosphere. *J Geophys Res* 107(D8): 4062. doi:10.1029/2001JD001216
- Sakazaki T, Fujiwara M, Zhang X, Hagan ME, Forbes JM (2012) Diurnal tides from the troposphere to the lower mesosphere as deduced from TIMED/SABER satellite data and six global reanalysis data sets. *J Geophys Res* 117:D13108. doi:10.1029/2011JD017117
- Sakazaki T, Sato K, Kawatani Y, Watanabe S (2015) Three-dimensional structures of tropical nonmigrating tides in a high-vertical-resolution general circulation model. *J Geophys Res Atmos* 120:1759–1775. doi:10.1002/2014JD022464
- Sasi MN, Krishnamurthy BV (1990) Diurnal and semidiurnal tides in the middle atmosphere over Balasore (21.5°N, 86.9°E). *J Atmos Sci* 47: 2101–2107
- Sasi MN, Ramkumar G, Deepa V (1998) Nonmigrating diurnal tides in the troposphere and lower stratosphere over Gadanki (13.5°N, 79.2°E). *J Geophys Res* 103:19485–19494
- Seidel DJ, Free M, Wang J (2005) Diurnal cycle of upper-air temperature estimated from radiosondes. *J Geophys Res* 110:D09102. doi:10.1029/2004JD005526
- Tsuda T, Nakamura T, Shimizu A, Yoshino T, Harijono SWB, Sribimawati T, Wiryo Sumarto H (1997) Observations of diurnal oscillations with a meteor wind radar and radiosondes in Indonesia. *J Geophys Res* 102(D22):26217–26224
- Tsuda T, Ratnam MV, May PT, Alexander MJ, Vincent RA, MacKinnon A (2004) Characteristics of gravity waves with short vertical wavelengths observed with radiosonde and GPS occultation during DAWEX (Darwin Area Wave Experiment). *J Geophys Res* 109: D20S03. doi:10.1029/2004JD004946
- Vincent RA, Kovalam S, Fritts DC, Isler JR (1998) Long term MF radar observations of solar tides in the low-latitude mesosphere: interannual variability and comparisons with the GSWM. *J Geophys Res* 103(D8):8667–8683
- Wallace JM, Patton DB (1970) Diurnal temperature variations: surface to 25 kilometers. *Mon Weather Rev* 98:548–552
- Williams CR, Avery SK (1996) Diurnal nonmigrating tidal oscillations forced by deep convective clouds. *J Geophys Res* 101(D2):4079–4091
- Wu DL, Jiang JH (2005) Interannual and seasonal variations of diurnal tide, gravity wave, ozone, water vapor as observed by MLS during 1991–1994. *Adv Space Res* 35:1999–2004
- Zhang X, Forbes JM, Hagan ME (2010a) Longitudinal variation of tides in the MLT region: 1. Tides driven by tropospheric net radiative heating. *J Geophys Res* 115: A06316. doi:10.1029/2009JA014897.
- Zhang X, Forbes JM, Hagan ME (2010b) Longitudinal variation of tides in the MLT region: 2. Relative effects of solar radiative and latent heating. *J Geophys Res* 115: A06317. doi:10.1029/2009JA014898.
- Zhang X, Forbes JM, Hagan ME (2011) Seasonal-latitude variation of the eastward-propagating diurnal tide with zonal wavenumber 3 in the MLT: influences of heating and background wind distribution. *J Atmos Terr Phys* 78–79:37–43. doi:10.1016/j.jastp.2011.03.005